

Imaging Polarization Interferometer for flat panel display characterization

Mathieu LUET, Pierre BOHER, Thierry LEROUX

ELDIM, 1185 rue d'Epron, 14200 Caen, France

Abstract

The next generation of MURATest will be able to make a hyper spectral analysis to get a high definition image with adjustable wavelength resolution. This paper introduces the principle of the new system, based on an imaging polarizing interferometer. The phase shift is realized by two symmetrical Wollaston prisms. The system produces an interference pattern directly on the CCD camera. The phase shift is linearly changed for all pixels using a mechanical translation.

1. Introduction

ELDIM is working on colorimetry since ten years. Its MURATest© equipment enables to measure the overall image characteristics of the display (uniformity, luminance and color). Based on a telecentric optics and a high resolution CCD sensor, it allows to measure the luminance and the color of the entire surface of displays. Up to now the color measurements have been based on color filters. For optimized accuracy, ELDIM uses up to 8 colors filters especially designed to match the photometric response of each CCD detector. In these conditions, accuracies of better than ± 0.002 CIE on (x,y) colorimetric coordinates can be demonstrated.

Nevertheless, for some specific applications, hyper spectral imaging is required instead of colorimetric measurements. This kind of technology has shown a lot of improvements these last few years. Different techniques can be used to get a spectral image. They can be classified in two great families. In the first kind, the spectrum is recorded directly with a direct imaging spectrometer. Prism or grating spectrometer with scanning slit, tunable Fabry-Perot filters [1], rocking interference filters or wedge filters [2], and rotating filter wheels are some practical examples of this solution. Their main drawback is the reduced efficiency for low radiance scenes and no or limited adaptability in terms of spectral resolution in addition to the mechanical complexity.

Indirect techniques in which an inversion of a measured intensity distribution is applied are generally much more efficient and tunable in terms of resolution. The standard configuration is exemplified by the Fourier Transform (FTS) imaging spectrometer which can reach efficiencies $> 90\%$ and a complete adaptability. One main drawback is generally related to their high sensitivity to vibrations and their limited angular aperture for imaging. Nevertheless, for high spectral imaging of low radiance scenes Fourier transform techniques offer potentially the best SNR but require stare stabilization for fully realize their potential [3].

In the proposed paper, we present an innovative Fourier transform imaging spectrometer based on a polarization interferometer built

with Wollaston prisms. This kind of optical mounting has already been developed for static FT spectrometers for gas analysis [4-9]. We apply for hyper spectral imaging for flat panel display application. In a first part, we present rapidly the principal of Fourier Transform spectrometers (FTS) and their advantages. A second part is devoted to the polarizing FTS and the characteristics of our optical mounting with simulation of the performance obtained by ray tracing algorithm.

2. Fourier Transform Spectrometer(FTS)

2.1. Michelson configuration

Wiener Khitchine theorem is the base of the FTS principle saying the spectrum distribution of a source $B(\sigma)$ can be extracted from the Fourier Transform of the interferogram. The most classical FTS instrument is the Michelson Interferometer as shown in figure 1. Two beams of light coming from the source are generated with a beam splitter and are reflected separately by one fixed and one moving mirror. After reflection they interfere on the detector. The phase shift is driven directly by the difference of optical pass between the two arms $\delta=d_1-d_2$. The interferogram is obtained by moving one mirror with a complex mechanism due to the required accuracy ($\sim \lambda/100$). This type of mounting is generally used in the infrared but is difficult to applied for shorter wavelengths.

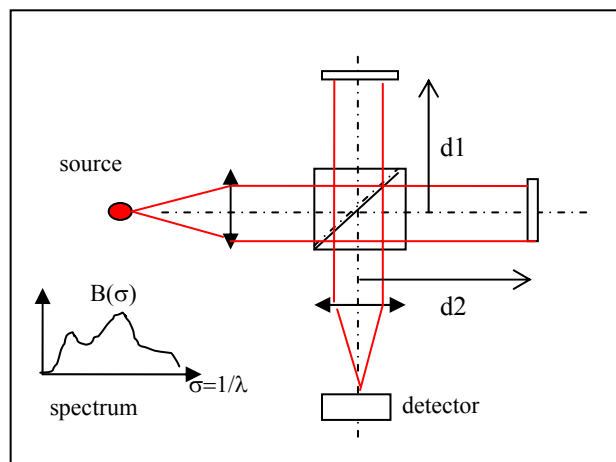


Figure 1 : Schematic of a Michelson Interferometer

The intensity measured by the detector is given by [11]:

$$I(\delta) = \int B(\sigma) \cos(2\pi\delta)d\sigma$$

Therefore, the distribution of the source is given by the Inverse Fourier Transform of the intensity:

$$B(\sigma) = \int I(\delta) \cos(2\pi\delta)d\delta$$

2.2. Resolution

The distance δ is finite so the spectrum B should be convolved with a Cardinal Sinus function which gives the resolution of the FTS [11]. Assuming a path difference δ between $-L$ and L and using an adequate apodization window the spectral resolution is approximately $\Delta\sigma=1/L$ [5]. The angular aperture α of the system is a limiting factor of the resolution. It can be defined usefully as the range of input angle over which the path difference does not vary by more than $\lambda/2$. Versus angle the path difference is given by $\delta=\delta_0 \text{ Cos}\alpha$. So, the angular condition is then [5]:

$$i \leq \sqrt{\frac{2\lambda}{L}}$$

In addition, to achieve this resolution, and reconstruct the Fourier Transform, we need enough number of measurements N with regards to the Nyquist criterion [11].

$$N \geq \frac{4}{\Delta\sigma\lambda_{\min}}$$

2.3. Advantages and drawbacks

Unlike classical spectrometer instruments, ~100% of the flux can be theoretically used in the FTS instruments. For flat panel display characterization, a resolution of about 10nm is required in the visible range (400nm – 800nm). In this case, $\delta\sigma = \delta\lambda/\lambda^2 = 3.3\text{e-}5/\text{nm}$ and so, about 300 acquisitions are enough theoretically in the FTS technique. Nevertheless, an important point for the FTS is that resolution is adjustable with the number of acquisition. The overall displacement of the Michelson should be at least $L=30\mu\text{m}$.

It leads to a maximum angular aperture around 6° to avoid correction. For 10nm resolution, the elemental movement of the mirror is about 100nm which is very small. Optical Elements positioning should then be very precise and very stable. That is why we suggest a more robust method using birefringent prisms, a new kind of polarization interferometer.

3. Polarization Interferometers

3.1. Principle

In this method, the phase shift is given by a birefringent element which acts as a polarizing beam splitter producing two diverging and orthogonally linearly polarized output rays (See figure 2a) [12]. The path difference δ between the two light rays is due to the propagation of the two rays at different speed. The polarization of the incoming beam is fixed by a first polarizer P1 (figure 2b). The second one, orthogonally positioned to P1, enables the two rays to spatially interfere. The big advantage

compared to the other FTS configurations is that the two rays follow spatially quasi the same optical path inside the same optical element. So, the sensitivity of this kind of device to the vibrations is very low. The price to pay is a reduction of the system efficiency below 50% due to the polarisers. This efficiency remains nevertheless much higher than those of direct imaging systems. The practical problem is as follow:

- Ensure that the rays interfere on the same plane where the CCD sensor will be located.
- Ensure that the device works for a given angular aperture (in practice $\sim \pm 10^\circ$).
- Find a way to change the path difference ($> \pm 30\mu\text{m}$) simultaneously on all the rays for the entire angular aperture.

In the following, we propose an optical configuration that fulfills all these requirements.

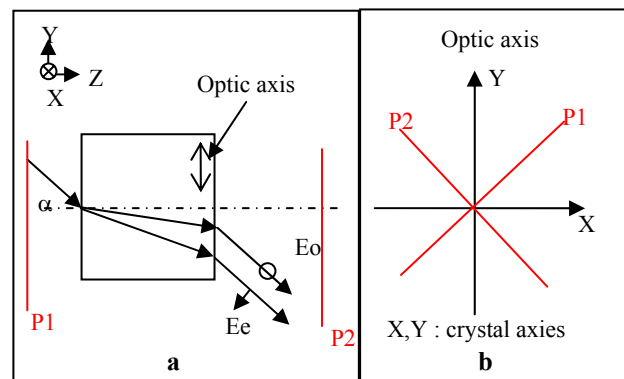


Figure 2 : Polarization interferometer principal

3.2. Double Wollaston prism configuration

Polarizing interferometers using Wollaston prisms are now commonly used for testing optical setup [13]. Most of the polarizing microscopes use birefringent prisms [13]. A Wollaston prism has two similar edges cemented and gives a spatial variable phase shift. The optic axes in the component wedges are parallel to the faces and mutually perpendicular [12]. The phase shift is different for different height h of rays (cf. figure 3a).

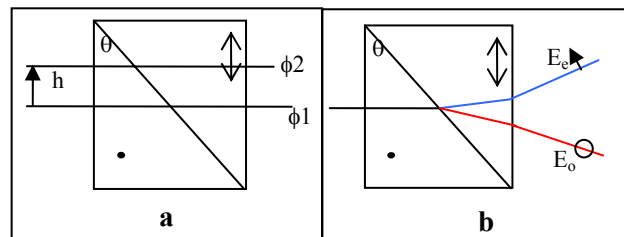


Figure 3 : Phase shift of a single Wollaston prism

θ is the angle of the wedge. n_e and n_o are the extraordinary and ordinary indices. In first approximation, the phase shift is given by:

$$\delta(h) = (n_e - n_o) 2 h \text{ Tan } \theta$$

The problem is that rays do not get out parallel in a simple Wollaston Prisms. To cope with the issue and have a more symmetrical configuration, it is necessary to add a second symmetrical Wollaston [4-10] (cf. figure 4). The wedge angle θ is the same for the two prisms, and x is the relative displacement of the prisms. In this case, the rays get out parallel whatever x and α . Double Wollaston prisms have already been involved in industrial instrument for gas detection [6] or as a laser wavemeter [7]. Nevertheless, these instruments do not make any imaging. The interferogram is collected spatially on a multichannel detector.

Our purpose is different because we want to make imaging using a CCD detector. So, the interference pattern is collected directly by the sensor and the path difference is changed by translating one Wollaston parallel to the other along the Y axis (see figure 4). In the following we have defined such a practical optical configuration and simulate its properties using a commercial ray tracing software [14].

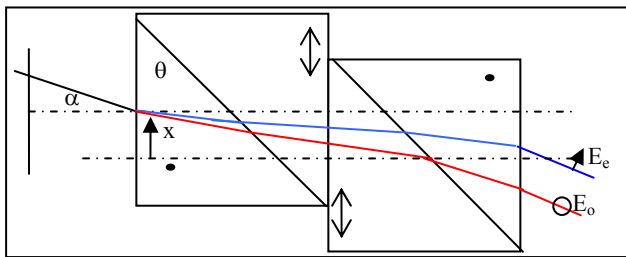


Figure 4 : The double Wollaston prism configuration

3.3. Ray tracing simulation

The two Wollaston prisms are made in magnesium fluoride that we have selected for its low dispersion. The tilt angle is $\theta=16^\circ$ and the translation is performed with a 25mm actuator. The system is mounted at the entrance of a ELDIM MURATest. The detection is made by a high resolution CCD cooled at -30°C . The phase shift for polarizing interferometers depends on two major parameters: the relative prisms position and the angular aperture. Each pixel of the camera (x,y) corresponds to a certain angle (α_x, α_y) as shown in figure 5.

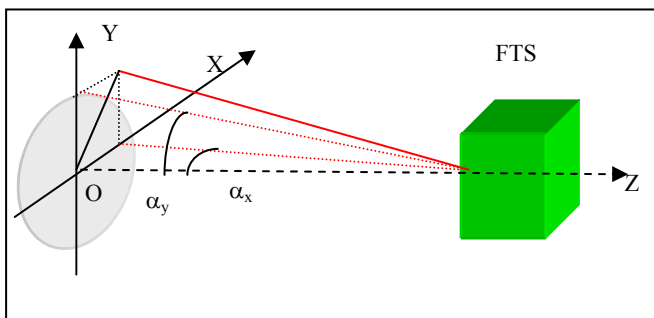


Figure 5 : Definition of the angular acceptance

An exact simulation has been necessary to characterize the system. The complete calculation is too complex but approximate solutions can be found for small angle α or with no tilt $\theta=0$. Miss Prunet has made the exact calculation of the phase different [9] but only in the plan YoZ. We have compared this analytical

solution with our computing results obtained with the ZEMAX software [14].

The intrinsic phase shift at $\lambda=500\text{nm}$ of the double Wollaston system in symmetric position ($x=0$), is reported in figure 6 for a practical angular acceptance of $\pm 10^\circ$. Also cross sections of the same quantities are reported in figure 7 with the exact calculation with the Prunet expressions [9].

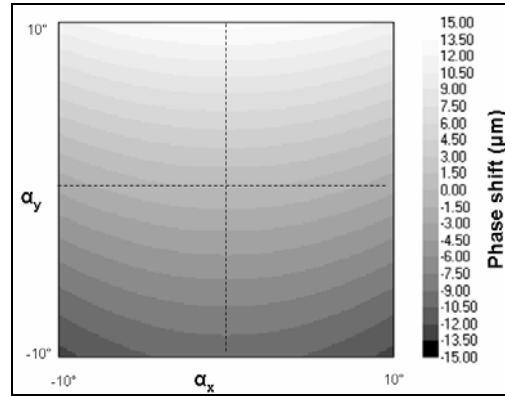


Figure 6: phase shift for $x=0\text{mm}$ and $\lambda=500\text{nm}$

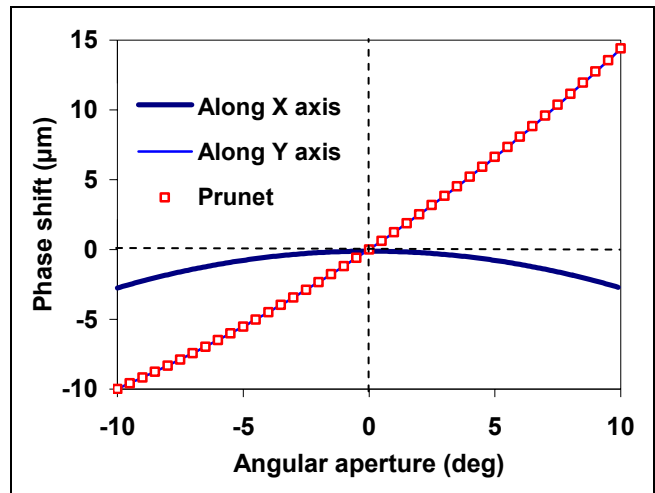


Figure 7: phase shift for the two cross sections of figure 6 and analytical results from reference [9]

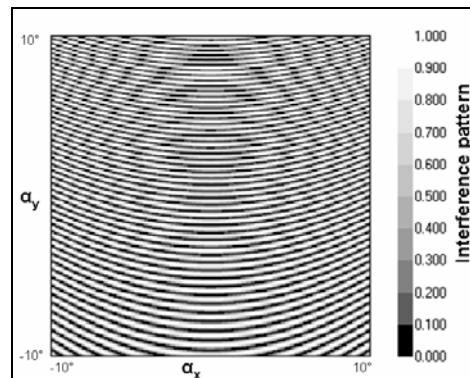


Figure 8: interference pattern at $x=0\text{mm}$ and $\lambda=500\text{nm}$

In the YoZ plane ($\alpha_x=0$) the phase shift depends strongly on the angular aperture. For $\alpha_y = 0$ is to say perfectly symmetric configuration the phase shift is $\delta=0\mu\text{m}$ as waited, but for $\alpha_y=-10^\circ$ and $\alpha_y = 10^\circ$ the phase shift is equal to $-10\mu\text{m}$ and $15\mu\text{m}$ respectively. The variation is more limited along the perpendicular axis XoZ but it is still non neglectable. It means that the interference pattern observed in monochromatic wavelength is an hyperboloid as one as already mention in the literature [13] and presents numerous interference fringes along the YoZ axis (cf. figure 8). The fringe pattern is tilted from the center due to the tilt angle of the Wollaston prisms. The phase shift versus prism position is linear and depends only on x for the normal incidence configuration. The fringe pattern is simply translated depending on the x position. The accuracy required on the translation is not very important (10mm for $65\mu\text{m}$). It is about 150 times less sensitive than the translation on a Michelson interferometer in the same conditions.

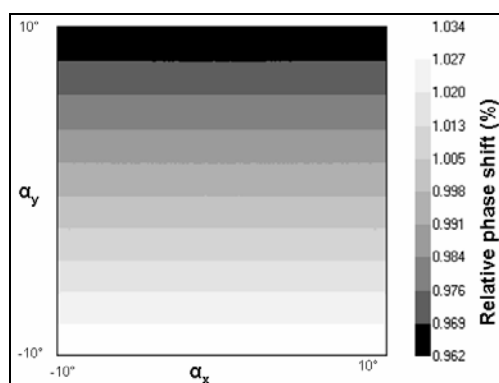


Figure 9: Relative phase shift due to prism position x

Nevertheless, as shown in figure 9, the phase shift produced by the prism translation depends on the angular aperture but only along the YoZ axis. This is not surprising since we have seen that we are above the maximum angular aperture (cf. 2.2). This dependence is easily corrected during the data analysis.

3.4. Chromatic dispersion

Even if MgF_2 is a low dispersion material a last imperfection of the system must be also corrected. The phase shift is not perfectly independent of λ (cf. figure 10). The difference in phase shift for 400nm and 800nm is less than $0.1\mu\text{m}$. A calibration is applied to correct this effect during Fourier transform analysis.

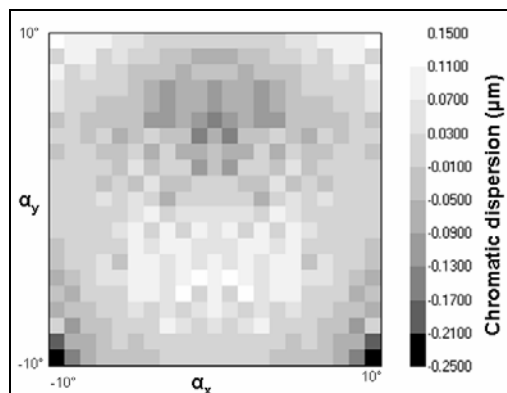


Figure 10: Chromatic dispersion between 400 and 800nm

4. Conclusion

We have presented a new innovating polarizing imaging interferometer. Its spectral resolution is as follows. The maximum translation is $\pm 12.5\text{mm}$ which produces a phase shift of $\Delta\text{max} = \pm 69\mu\text{m}$ so $\Delta\sigma = 0.014\mu\text{m}^{-1}$. The maximum spectral resolution is then $\Delta\lambda = 4\text{nm}$ at 550nm and a minimum of $N=700$ acquisitions is required. For 10nm resolution about 120 acquisitions will required which will take a short time with MURATest instrument.

7. References

- [1] J. Oleson, R. Jungquist, Z. Ninkov, "Tuneable multispectral imaging system technology for airborne applications", SPIE 2480, 268, 1995
- [2] J.C. Demro, R. Hartsorne, L.M. Woody, P.A. Levine, J.R. Tower, "Design of a multispectral wedge filter remote sensing instrument incorporating a multipoint thinned CCD array", SPIE 2480, 280, 1995
- [3] A.R. Harvey, J. Beale, A.H. Greenaway, T.J. Hanlon, J. Williams, "Technology options for imaging spectrometry", SPIE 4132, 13, 2000
- [4] M. Padgett, A. Harvey, "A static FTS based on Wollaston Prisms", Rev. Sci. Instr., 66, 2807, 1995
- [5] J. Courtial, B. Patterson, A. Harvey, W. Sibbett, M. Padgett, "Design of a static FTS with increased field of view", Appl. Opt., 35, 6698, 1996
- [6] S. Padgett, "Gasoline analysis and brand identification using a static FTS UV", Applied Optics, 1999
- [7] D. Steers, W. Sibbett, M. Padgett, "Dual purpose compact spectrometer and fiber coupled laser wavemeter based on Wollaston prisms", Appl. Opt., 37, 5777, 1998
- [8] S. Prunet-Cassan, « Conception et réalisation d'un spectromètre par TF », Thesis, Ecole Nationale Supérieure, November 2000
- [9] S. Prunet, B. Journet, G. Fortunato, « Exact calculation of the optical path difference and description of a new birefringent interferometer », Opt. Eng., 38, 983, 1999
- [10] D. Fletcher-Homes, A. Harvey, "Birefringent Fourier Transform imaging spectrometer", SPIE 4816, 46, 2002
- [11] S. Davis, M. Abrams, J. Brault, "Fourier Transform Spectrometry", Academic Press, 2001
- [12] Serge Huard, « Polarisation de la Lumière », MASSON, 1994
- [13] M. Françon, S. Mallick, "Polarization Interferometers: Applications in Microscopy and Macroscopy", Wiley Interscience, New York, 1971
- [14] Zemax Software 3 mars 2004